Bioorganic & Medicinal Chemistry Letters 20 (2010) 330–333

Contents lists available at ScienceDirect

Bioorganic & Medicinal Chemistry Letters

journal homepage: www.elsevier.com/locate/bmcl

2,4-Diaminopyrimidine MK2 inhibitors. Part I: Observation of an unexpected inhibitor binding mode

Maria A. Argiriadi, Anna M. Ericsson, Christopher M. Harris, David L. Banach, David W. Borhani [†], David J. Calderwood, Megan D. Demers [‡], Jennifer DiMauro, Richard W. Dixon [§], Jennifer Hardman, Silvia Kwak, Biqin Li, John A. Mankovich, Douglas Marcotte [¶], Kelly D. Mullen, Baofu Ni, M. Pietras, Ramkrishna Sadhukhan, Silvino Sousa, Medha J. Tomlinson, Lu Wang, Tao Xiang, Robert V. Talanian [*]

Abbott Laboratories, 100 Research Drive, Worcester, MA 01605-5314, USA

ARTICLE INFO

Article history:
Received 18 August 2009
Revised 21 October 2009
Accepted 26 October 2009
Available online 29 October 2009

Keywords:
MAPKAP-K2
MK2
TNFα
Diaminopyrimidine

ABSTRACT

MK2 is a Ser/Thr kinase of significant interest as an anti-inflammatory drug discovery target. Here we describe the development of in vitro tools for the identification and characterization of MK2 inhibitors, including validation of inhibitor interactions with the crystallography construct and determination of the unique binding mode of 2,4-diaminopyrimidine inhibitors in the MK2 active site. Use of these tools in the optimization of a potent and selective inhibitor lead series is described in the accompanying Letter.

Tumor necrosis factor-α (TNFα) is a potent pro-inflammatory cytokine with a crucial signaling role in the cellular pathogenic mechanisms of rheumatoid arthritis (RA) and related autoimmune diseases.[1] TNFα-binding biologics such as etanercept, infliximab, and adalimumab demonstrate dramatically enhanced safety and efficacy in RA and related diseases compared to prior treatments.[2]

Inhibition of TNFα production and signaling mechanisms with oral drugs may also be efficacious in RA. Prominent among these is the p38 mitogen-activated protein kinase. Many p38 inhibitors with promising preclinical properties have been reported, but none have achieved clinical success.[3] The Ser/Thr kinase Mitogen Activated Protein Kinase Activated Protein Kinase 2 (MAPKAP-K2 or MK2) is a p38 substrate whose activity may fully account for the pro-inflammatory effects of p38.[4,5] MK2-deficient mice are viable and fertile, and defective in TNFα production.[6] Splenocytes from these animals are defective in TNFα, IL-6, and IFNγ production,[6] and the animals are resistant to collagen-induced arthritis.[7] Dosed orally in rats, MK2 inhibitors can block acute systemic induction of TNFα by lipopolysaccharide[8] and can reduce paw swelling in the streptococcal cell wall arthritis model.[9]

Few potent and specific inhibitors of MK2 have been described. None to our knowledge have been tested clinically. Here we describe in vitro tools to characterize MK2 inhibitors and enable structure-based lead design. In the accompanying Letter,[10] we describe structure-based optimization of the enzymatic and cellular inhibition properties of a series of 2,4-diaminopyrimidine MK2 inhibitors.

To prepare active MK2 for inhibitor profiling, we phosphorylated recombinant human MK2 by incubation with recombinant p38α and ATP.[11] Using a kinase activity assay,[12,13] we confirmed that full MK2 catalytic activity required phosphates at Thr222, Ser272, and Thr334 as reported.[14] MK2(36–400) had the greatest activity and was used for inhibitor screening. MK2(47–366) and MK2(41–364) were about 100- and 1000-fold less active than MK2(36–400) after p38α activation, respectively. These losses may be due to exposure of the auto-inhibitory sequence (residues 328–364) in the absence of the nuclear export signal (364–368) and the C-terminal nuclear localization sequence (373–389).[15,16] For MK2(47–366), Thr222Glu or Thr334Glu 'activating' mutations gave no activity boost.

Our best crystallization was with MK2(41–364) and MK2(47–366)Thr222Glu, both nonphosphorylated and so catalytically inactive.[12] We could not crystallize any active, phosphorylated construct. Since crystallized constructs were inactive, we could not validate ligand binding using enzyme inhibition, and so could not be sure that structure-based optimization would lead to better

* Corresponding author. Tel.: +1 508 849 2581.
E-mail address: bob.talanian@abbott.com (R.V. Talanian).
† Present address: DE Shaw Research, NY 10036, USA.
‡ Present address: Descher LLC, Raleigh, NC 27607, USA.
§ Present address: Vertex Pharmaceuticals, Cambridge, MA 02139, USA.
¶ Present address: Biogen Idec, Cambridge, MA 02142, USA.

0960-894X/$ - see front matter © 2009 Elsevier Ltd. All rights reserved.
doi:10.1016/j.bmcl.2009.10.102

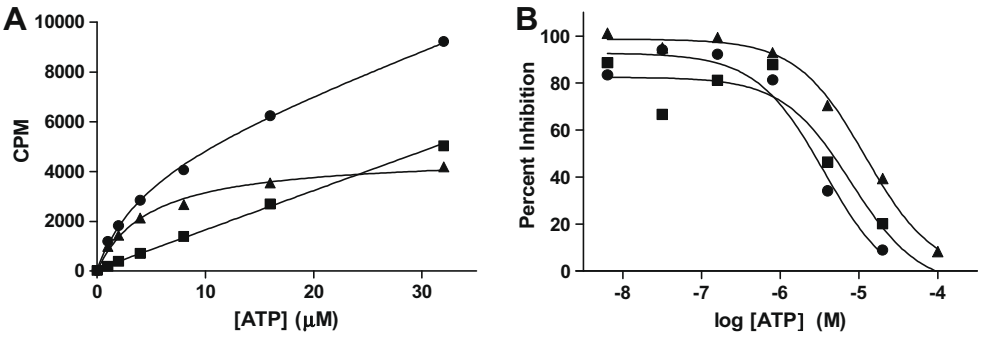

Figure 1. MK2 ATP competition binding assay. (A) [8-^{3}H] ATP titration of phosphorylated MK2(36–400). Specific binding (▲), total binding (●), non specific binding with 5 mM ATP (■), K_D = 4.8 μM. B, [8-^{3}H] ATP binding competition by unlabeled ATP. Phosphorylated MK2(36–400) (●), nonphosphorylated MK2(36–400) (■), nonphosphorylated MK2(41–364) (▲). IC_{50} values are shown in Table 1.

enzyme inhibitors. The ATP sites of inactive protein kinases are commonly distorted or blocked. For example, the ATP site of insulin receptor kinase is occluded by its unphosphorylated activation loop, blocking entry of ATP site-directed inhibitors.[17] To correlate ligand binding to inactive MK2 constructs with enzyme inhibition, we developed a radioligand binding assay to measure MK2 ligand binding directly. Inhibitor competition with ATP was measured in a Scintillation Proximity Assay (SPA), in which MK2-bound [8-^{3}H]ATP capture to a glutathione-conjugated scintillant bead reports MK2 ATP site ligand binding.[18] Figure 1A shows the ATP binding isotherm for activated MK2(36–400); competition with unlabeled ATP is shown in Figure 1B. SPA also worked well for nonphosphorylated MK2(36–400) and MK2(41–364) (Fig. 1B). All assays had good Z′ values (Table 1). The phosphorylated enzyme ATP affinity, as measured by ATP K_D or IC_{50}, was similar to the ATP K_M. Also, the MK2 ATP affinity changed only modestly in the nonphosphorylated enzymes or with C-terminal truncation, indicating preservation of the ATP binding site in all cases. Competitive binding IC_{50} values for a series of ATP-competitive MK2 inhibitors[10] aligned well with activity assays (Fig. 2A). The MK2 inhibitor affinities for nonphosphorylated MK2(36–400) (Fig. 2B) or MK2(41–364) (not shown) were also preserved.

Table 1
MK2 ATP competition assay parameters

Parameter	Phospho-MK2 (36–400)		MK2(36–400) SPA	MK2(41–364) SPA
	HTRF	SPA		
Z′	0.9	0.70	0.40	0.70
ATP K_M (μM)	1.9	N.A.	N.A.	N.A.
ATP K_D (μM)	N.A.	4.8	N.D.	26
ATP IC_{50} (μM)	N.A.	2.8	6.3	12
Staurosporine IC_{50} (μM)	0.70	0.66	1.7	3.4

N.A., not applicable; N.D., not determined.

MK2 is closely related in structure and mechanism to cAMP-dependent protein kinase (PKA)[19] and Ca^{2+}/calmodulin dependent protein kinase (cAMK).[20] These kinases feature unusual regulatory elements: a C-terminal segment (MK2), an additional subunit (PKA), or a separate protein (cAMK). In inactive MK2, the C-terminal autoinhibitory α-helix occludes substrate binding, but does not block ATP binding site access. Our binding data confirm preservation of both the ATP binding site (Fig. 1) and the structure–activity relationship (SAR) of a series of ATP-competitive inhibitors across MK2 constructs. The SPA assay could also be useful for accurate measurement of inhibitor potency toward a nonphosphorylated tyrosine kinase, for which auto-phosphorylation during activity assays may complicate potency determination.

Several forms of recombinant MK2 were crystallized with inhibitors. These methods were described in a recent study in which pseudoactivating mutations were introduced into the protein scaffold to obtain novel crystal forms.[12] Our first MK2 crystal structure was determined using such a construct (MK2(47–366)Thr222Glu). Subsequent structures were determined using a previously reported construct under novel crystallization conditions (MK2(41–364)).[12,21]

Inhibitor optimization started with 2-amino-4-(4-hydroxyphenyl)aminopyrimidine (**1**) (Fig. 3). Given the many reports of diaminopyrimidines as potent hinge binding elements for many kinases (e.g., CDK[22] or FAK[23]), and the lack of reports of phenols as hinge binding elements (we are aware only of reports of polyhydroxyaromatics such as flavopiridol[24] as kinase inhibitors), we expected that the diaminopyrimidine ring system would make typical hinge interactions with MK2. In particular, the 2-amino

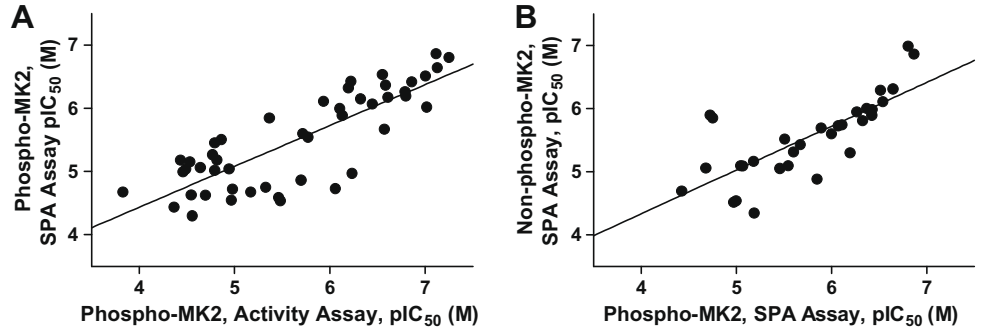

Figure 2. (A) Validation of SPA method with HTRF assay. For linear fit, $y = 0.65x + 1.9$, $r^2 = 0.67$. (B) Validation of unphosphorylated MK2 construct with SPA assay. For linear fit, $y = 0.69x + 1.6$, $r^2 = 0.57$.

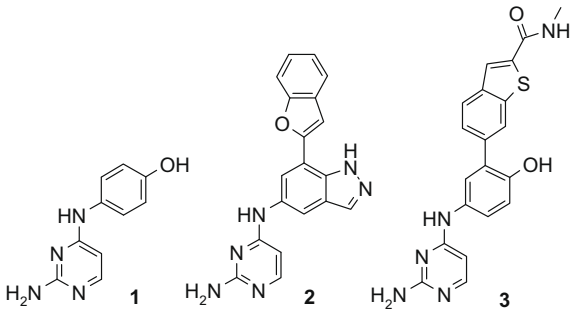

Figure 3. 2,4-Diaminopyrimidine MK2 inhibitors.

group and the ring N3 nitrogen atom were expected to form a donor–acceptor pair with hinge residues Glu139 and Leu141. In this model the phenol of **2** or **3**, respectively, would lie near the DFG motif.

Our structures of indazole **2** (co-crystal) and phenol **3** (soaked crystal) bound to MK2(41–364) and MK2(41–364)Thr222Glu, respectively,[25] revealed an unanticipated reversed binding mode, with several interesting features (Fig. 4).

SAR indicated that both pyrimidine nitrogen atoms were crucial to potency (not shown). The MK2(41–364)Thr222Glu/**3** complex crystal structure revealed an intricate hydrogen-bonding network between the N1 and N3 atoms of the inhibitor and MK2 residues Lys93 (catalytic lysine) and Thr206 (precedes DFG motif) (Fig. 4b). The Thr206 side chain rotated to engage the N3 atom. Also, a well-ordered water molecule was bound in the hydrophilic pocket behind Met138. This water was tetrahedrally coordinated by Glu104 (αC), His108 (αC), the backbone NH of Asp207 (DFG), and the inhibitor 2-amino group (Fig. 4b).

Both indazole **2** and phenol **3** made additional hydrogen-bonding interactions with the Leu141 backbone NH, in the center of the hinge region (Fig. 4a and c). In the indazole series, an additional hinge hydrogen bond was seen between the indazole and the Leu141 backbone carbonyl (Fig. 4c). The indazole 7- or phenol 2-substituents were in van der Waals contact with the distal hinge region. Phenol **3** made an interaction between the amide NH and the hinge residue Asp142 side chain (Fig. 4a). In the MK2/**2** co-crystal structure, the glycine-rich loop adopted a conformation typical of 'active' MK2. In contrast, the loop adopted an 'inactive' conformation in the (soaked) MK2/**3** structure. It is unclear whether this flexibility is driven by inhibitor binding or crystallization. As seen in other MK2 structures, this region of MK2 displays significant mobility and may be a key area for inhibitor design.

Figure 4c shows active site regions targeted to improve inhibitor potency. Indazole 7-substituents were varied near the distal hinge. Due to the proximity to solvent, alterations here might also permit modulating solubility and pharmacokinetic properties. In many MK2/inhibitor complexes, a water molecule was tetrahedrally coordinated in the hydrophobic pocket behind Met138. Replacement of this water would allow an MK2 inhibitor access beyond the gatekeeper residue. Another region of optimization was the glycine-rich loop, with the goal of engaging the loop in hydrogen-bond interactions to stabilize its flexibility. Several MK2 structures, determined as both active and inactive forms, have demonstrated the plasticity of this loop.[21,26] Inhibitor design could clamp the loop in place and prevent this conformational change.[26] Another region was the ribose pocket, to engage Glu145 and Glu190.

Structural study and in vitro analysis of MK2 inhibitor potency permitted understanding of inhibitor binding modes and identified key interaction points in the active site. A comprehensive structure-based design strategy was developed based on these observations and is presented in Part II.[10]

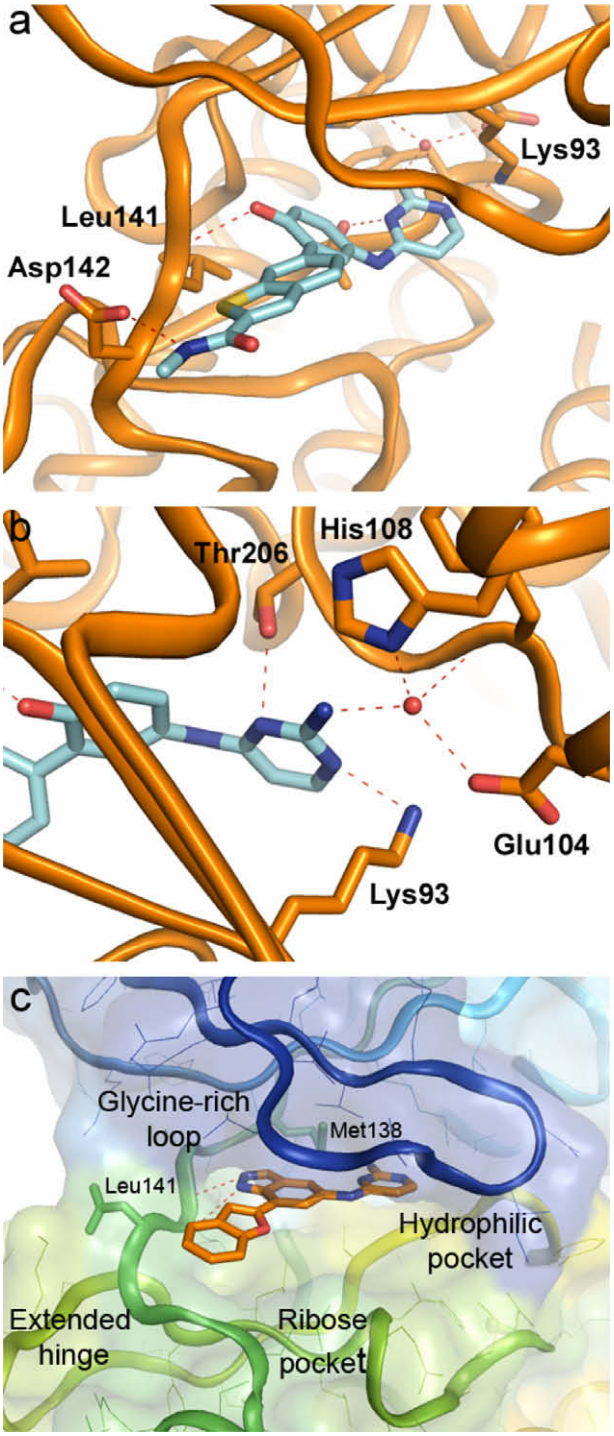

Figure 4. (a) MK2/phenol **3** complex. The phenol hydrogen bonds to Asp142 and hinge residue Leu141. (b) The diaminopyrimidine interacts with Lys93, Thr206, Glu104, His108, and a bound water molecule. (c) MK2/indazole **2** complex, showing the conserved binding mode including hinge interactions with Leu141. Inhibitor optimization regions are identified.

Acknowledgments

The authors thank Kristine Frank and Kent Stewart for careful readings of the Letter.

Supplementary data

Supplementary data associated with this article can be found, in the online version, at doi:10.1016/j.bmcl.2009.10.102.

References and notes

1. Goldstein, D. M.; Gabriel, T. *Curr. Top. Med. Chem.* **2005**, *5*, 1017.
2. Feldmann, M.; Brennan, F. M.; Foxwell, B. M.; Taylor, P. C.; Williams, R. O.; Maini, R. N. *J. Autoimmun.* **2005**, *25*, 26.
3. McInnes, I. B.; Schett, G. *Nat. Rev. Immunol.* **2007**, *7*, 429.
4. Gaestel, M.; Kotlyarov, A.; Kracht, M. *Nat. Rev. Drug Disc.* **2009**, *8*, 480.
5. Mbalaviele, G.; Monahan, J. B. *Expert Opin. Drug Discovery* **2008**, *3*, 163.
6. Kotlyarov, A.; Neininger, A.; Schubert, C.; Eckert, R.; Birchmeier, C.; Volk, H. D.; Gaestel, M. *Nat. Cell Biol.* **1999**, *1*, 94.
7. Hegen, M.; Gaestel, M.; Nickerson-Nutter, C. L.; Lin, L.-L.; Telliez, J.-B. *J. Immunol.* **2006**, *177*, 1913.
8. Anderson, D. R.; Meyers, M. J.; Vernier, W. F.; Mahoney, M. W.; Kurumbail, R. G.; Caspers, N.; Poda, G. I.; Schindler, J. F.; Reitz, D. B.; Mourey, R. J. *J. Med. Chem.* **2007**, *50*, 2647.
9. Mourey, R. J.; Anderson, G.; Hirsch, J.; Meyers, M.; Mnich, S.; Stillwell, L.; Thiede, M.; Vernier, W.; Webb, E.; Zhang, J.; Gaestel, M.; Monahan, J. In *Pharmacological characterization of a small molecule inhibitor of MAPKAP kinase-2 (MK-2) for the inhibition of TNFα production*; 14th International Conference of the Inflammation Research Association, Cambridge, MD, 2006.
10. Harris, C. M.; Ericsson, A. M.; Argiriadi, M. A.; Barberis, C.; Borhani, D. W.; Burchat, A.; Calderwood, D. J.; Cunha, G. A.; Dixon, R. W.; Frank, K. E.; Johnson, E. F.; Kamens, J.; Kwak, S.; Li, B.; Mullen, K. D.; Perron, D. C.; Wang, L.; Wishart, N.; Wu, X.; Zhang, X.; Zmetra, T. R.; Talanian, R. V. *Bioorg. Med. Chem. Lett.* (2009), doi:10.1016/jbmcl.2009.10.103.
11. To measure the effect of p38 activation, nonphosphorylated MK2 samples were assayed with and without 2 ng active p38α (upstate, no 14-251). Separate experiments demonstrated that p38α does not activate the MK2 assay peptide substrate (not shown).
12. Argiriadi, M. A.; Sousa, S.; Banach, D.; Marcotte, D.; Xiang, T.; Tomlinson, M. J.; Demers, M.; Harris, C.; Kwak, S.; Hardman, J.; Pietras, M.; Quinn, L.; DiMauro, J.; Ni, B.; Mankovich, J.; Borhani, D. W.; Talanian, R. V.; Sadhukhan, R. *BMC Struct. Biol.* **2009**, *9*, 16.
13. Jia, Y.; Quinn, C. M.; Gagnon, A.; Talanian, R. *Anal. Biochem.* **2006**, *356*, 273.
14. Ben-Levy, R.; Leighton, I. A.; Doza, Y. N.; Attwood, P.; Morrice, N.; Marshall, C. J.; Cohen, P. *EMBO J.* **1995**, *14*, 5920.
15. Ben-Levy, R.; Hooper, S.; Wilson, R.; Paterson, H. F.; Marshall, C. J. *Curr. Biol.* **1998**, *8*, 1049.
16. Engel, K.; Kotlyarov, A.; Gaestel, M. *EMBO J.* **1998**, *17*, 3363.
17. Hubbard, S. R.; Wei, L.; Ellis, L.; Hendrickson, W. A. *Nature* **1994**, *372*, 746.
18. Bosworth, N.; Towers, P. *Nature* **1989**, *341*, 167.
19. Zheng, J.; Knighton, D. R.; ten Eyck, L. F.; Karlsson, R.; Xuong, N.; Taylor, S. S.; Sowadski, J. M. *Biochemistry* **1993**, *32*, 2154.
20. Goldberg, J.; Nairn, A. C.; Kuriyan, J. *Cell* **1996**, *84*, 875.
21. Underwood, K. W.; Parris, K. D.; Federico, E.; Mosyak, L.; Czerwinski, R. M.; Shane, T.; Taylor, M.; Svenson, K.; Liu, Y.; Hsiao, C. L.; Wolfrom, S.; Maguire, M.; Malakian, K.; Telliez, J. B.; Lin, L. L.; Kriz, R. W.; Seehra, J.; Somers, W. S.; Stahl, M. L. *Structure* **2003**, *11*, 627.
22. Chu, X. J.; DePinto, W.; Bartkovitz, D.; So, S. S.; Vu, B. T.; Packman, K.; Lukacs, C.; Ding, Q.; Jiang, N.; Wang, K.; Goelzer, P.; Yin, X.; Smith, M. A.; Higgins, B. X.; Chen, Y.; Xiang, Q.; Moliterni, J.; Kaplan, G.; Graves, B.; Lovey, A.; Fotouhi, N. *J. Med. Chem.* **2006**, *49*, 6549.
23. Roberts, W. G.; Ung, E.; Whalen, P.; Cooper, B.; Hulford, C.; Autry, C.; Richter, D.; Emerson, E.; Lin, J.; Kath, J.; Coleman, K.; Yao, L.; Martinez-Alsina, L.; Lorenzen, M.; Berliner, M.; Luzzio, M.; Patel, N.; Schmitt, E.; LaGreca, S.; Jani, J.; Wessel, M.; Marr, E.; Griffor, M.; Vajdos, F. *Cancer Res.* **2008**, *68*, 1935.
24. Baumli, S.; Lolli, G.; Lowe, E. D.; Troiani, S.; Rusconi, L.; Bullock, A. N.; Debreczeni, J. E.; Knapp, S.; Johnson, L. N. *EMBO J.* **2008**, *27*, 1907.
25. Structures of MK2 complexed with **2** and **3** were solved to 2.9 Å resolution each, and R_{free} 29.7 and 26.5, respectively. The coordinates for the crystal structures of MK2/**2** and MK2/**3** are deposited in the Protein Data Bank with IDs 3KC3 and 3KA0, respectively. Full details of crystal data collection, structure determination and a table of structure statistics are in Supplementary data.
26. Meng, W.; Swenson, L. L.; Fitzgibbon, M. J.; Hayakawa, K.; ter Haar, E.; Behrens, A. E.; Fulghum, J. R.; Lippke, J. A. *J. Biol. Chem.* **2002**, *277*, 37401.